Communication in Physical Sciences, 2025, 12(2) 674-685

Probing the Effects of Atomic Position Changes on the Structural, Electronic, and Thermoelectric Properties of Alpha Phase of Half-Heusler ZrPtPb Compound: A First-Principles Study

Funmilayo Ayedun
Received: 12 November 2024/Accepted: 04 March 2025/Published: 13 March 2025
https://dx.doi.org/10.4314/cps.v12i3.2

Abstract: *The structural and electronic responses of two* α*-phases of ZrPtPb compound were considered by employing Perdew-Burke-Ernzehof-Projected - Augmented-Wave (PBE-PAW) Generalized Gradient Approximation(GGA) based on Density Functional Theory as exchange correlation function found in Quantum Espresso code. The thermoelectric properties of ZrPtPb were investigated to evaluate its suitability for high-temperature energy conversion applications through semi-classical Boltzmann Transport equations. The study examined the Seebeck coefficient, electrical conductivity, power factor, and figure of merit (ZT) for both p-type and n-type configurations. The results indicate that p-type ZrPtPb exhibits superior thermoelectric performance, with a Seebeck coefficient reaching 6.65 μV/K at 800K and a peak power factor of 6.57 × 10^{10}W/msK². The figure of merit (ZT) for the p-type material consistently exceeds 1, with a maximum value of 6.52 at 800K, confirming its strong potential for waste heat recovery. This study also reported a high electronic fitness function (EFF) of 0.92194 × 10^{-19} $W^{5/3}ms^{-1/3}K^{-2}$ at 800K, further supporting the efficiency of hole conduction over electron conduction in ZrPtPb. The alignment of these trends suggests that the material's thermoelectric properties are robust and reproducible. With its increasing efficiency at higher temperatures, ZrPtPb remains a strong candidate for advanced thermoelectric applications. Further optimization of doping concentrations and microstructural properties could enhance its performance, positioning it as a leading material for sustainable energy conversion technologies.*

Keywords: *Atomic positions, Density Functional Theory, Thermoelectricity, half – Heusler, Generalized Gradient Approximation.*

Funmilayo Ayedun
Department of Physics, National Open University of Nigeria
Jabi, FCT, Abuja
Email: fayedun@noun.edu.ng
Orcid id: 0000-0001-5421-9305

1.0 Introduction

Half-Heusler (HH) compounds have emerged as a class of materials with significant promise for thermoelectric applications due to their unique structural, electronic, and transport properties. These materials are characterized by a distinctive XYZ structure, where X and Y are transition metals, and Z is a main-group element, forming a ternary intermetallic system with a cubic MgAgAs-type crystal structure (Felser et al., 2015). Due to their inherent band structure tunability, HH compounds exhibit favorable thermoelectric properties such as high Seebeck coefficients, moderate electrical conductivity, and low thermal conductivity, making them ideal candidates for energy conversion applications (Zhu et al., 2023).

The importance of investigating atomic position variations in HH compounds lies in their profound influence on structural stability, electronic band structure, and thermoelectric efficiency. The modification of atomic positions within the crystal lattice can induce changes in electronic density of states, carrier concentration, and phonon scattering mechanisms, thereby optimizing the material's Figure of merit (Yin et al., 2024). Previous studies have demonstrated that atomic substitutions and positional

modifications within HH structures enhance their thermoelectric performance by improving carrier mobility and reducing lattice thermal conductivity (Khatri & Adhikari, 2023; Bamgbose, 2020). Therefore, understanding the effects of atomic position variations is crucial for advancing the development of high-performance HH thermoelectric materials.

Recent studies on HH compounds have focused on various aspects of their structural, electronic, and thermoelectric properties. For example, Serrano-Sanchez et al. (2020) investigated the thermoelectric properties of n-type HH NbCoSn with Pt substitution and observed enhanced power factors. Dong et al. (2022) explored HH-like compounds with tunable p- to n-type conductivity, demonstrating the significance of atomic configurations in dictating transport properties. Mitra et al. (2022) further advanced state-of-the-art thermoelectric performance in conventional HH alloys by optimizing atomic arrangements. Kaur & Kaur (2017) conducted a first-principles study on the thermoelectricity of ScRhTe and ZrPtPb HH compounds, highlighting the potential of ZrPtPb for thermoelectric applications. However, despite these advances, a detailed investigation into the impact of atomic position variations on ZrPtPb remains lacking.

The knowledge gap in existing literature pertains to the absence of comprehensive first-principles investigations into how atomic position variations influence the structural stability, electronic properties, and thermoelectric efficiency of ZrPtPb HH compounds. Most prior studies have primarily focused on compositional tuning rather than precise atomic positional effects. This research aims to bridge this gap by utilizing Density Functional Theory (DFT) calculations to explore the structural stability, electronic band structure, and thermoelectric properties of ZrPtPb in different atomic configurations. This study looks into two α – phases with Wycoff positions XYZ; Zr:(0.50, 0.50, 0.50), Pb:(0.25, 0.25, 0.25), Pt: (0.00, 0.00,0.00) and ZYX; Zr:(0.00, 0.00,0.00), Pb:(0.25, 0.25, 0.25), Pt: (0.50, 0.50, 0.50). The significance of this study lies in its potential to provide insights into the optimization of HH materials for thermoelectric applications, thereby contributing to the development of more efficient thermoelectric devices.

The objective of this study is to analyze the effects of atomic position variations on the structural, electronic, and thermoelectric properties of the ZrPtPb HH compound using first-principles calculations. Specifically, the study aims to determine the most stable atomic configuration, evaluate the influence of atomic position on electronic band structure and density of states, and assess the impact on thermoelectric parameters such as electrical conductivity, Seebeck coefficient, and power factor. By elucidating these aspects, this research will contribute to a deeper understanding of HH compounds and their optimization for practical applications in thermoelectric energy conversion.

2.0 Computational Approach

In this research, the nonlinear core correction scalar relativistic PBE-PAW exchange and correlation functional within the generalized gradient approximation (GGA) was employed using the Quantum ESPRESSO library (Giannozzi et al., 2009, 2017). This approach was selected due to its accuracy, as well as its computational time and cost efficiency (Perdew et al., 1992, 2008). The minimized k-point, energy cutoff, and lattice parameter were relaxed and self-consistently calculated, with a convergence threshold of 0.01 mRy for both structural and electronic computations using smearing occupation. The kinetic energy cutoff for self-consistent calculations was fixed at 80 Ry.

An 8 × 8 × 8 k-point sampling grid was employed using the Monkhorst-Pack method (Monkhorst& Pack, 1976), while a denser 32 × 32 × 32 k-point was used for density of states calculations. To analyze transport properties, semi-classical Boltzmann transport equations, as implemented in the BoltzTrap package, were applied (Madsen & Singh, 2006). The electronic fitness function

(EFF) was evaluated using the TransM code (Xing et al., 2017).

3.0 Results and discussion

3.1 Structural and Electronic Properties

The optimized lattice parameters, ground state energy at various volumes were calculated for the conventional face centred cubit unit cells of two alpha phases of ZrPtPb compound. Fermi energy level which aids in appraisal of density of electrons, quantity of holes in the material and it commensurate holes and density with regard to temperature was also examined. The varied volumes (V) and energy (E) were fit into third- order Birch-Munarghan equation of state as expressed in equation (1). The relaxed lattice parameters, bulk moduli, pressure derivatives and Fermi energy were recorded in Table 1. The stable phase out of these two is α_1 (XYZ). The ground total lattice constant for α_1 (ZYX) is in excellent agreement with the experimental data by Gautier and his co-researchers (Gautier et *al*., [17].

$$\delta E(V) = E - E_0 = BV_0\left[\frac{V_n}{B'}\right] + \left(\frac{1}{(1-B')}\right) + \left(\frac{V_n}{B'(B'-1)}\right) \quad (1)$$

where E_o is the equilibrium energy, V_o is equilibrium volume, B is the bulk modulus and B' is the pressure derivative.

Table 1 also presents the structural and electronic properties of the investigated α_1 (XYZ) and α_2 (ZYX) structures, including their relaxed lattice constants, bulk modulus, pressure derivative of the bulk modulus, minimum energy, Fermi energy, and band energy gap. The relaxed lattice constant for α_1 (XYZ) is 6.508 Å, while for α_2 (ZYX), it is 6.514 Å. These values closely align with previously reported values of 6.537 Å and 6.518 Å, suggesting that the structural optimization performed in this study is consistent with established literature data.

The bulk modulus, which represents the material's resistance to volume change under pressure, is relatively low for both structures, with α_1 having a bulk modulus of 0.500 GPa and α_2 having 0.499 GPa. This indicates that both structures are relatively soft and easily compressible. The pressure derivative, B′, is slightly higher for α_1 at 2.19GPa compared to 1.92GPa for α_2, implying a minor difference in their response to external pressure variations.

The minimum energy for α_1 (XYZ) is -1990.54903 Ry, while for α_2 (ZYX), it is slightly lower at -1991.10883 Ry. The lower minimum energy of α_1 suggests that it is energetically more stable than α_2, making α_1 the more favorable phase under the given computational conditions. The Fermi energy, which represents the highest occupied electronic state at absolute zero temperature, is 13.6880 eV for α_1 and 13.7303 eV for α_2. The slightly higher Fermi energy of α_2 indicates a marginally greater electron density at the Fermi level, which could influence its electronic and transport properties.

The calculated band gaps indicate semiconducting behavior for both phases. The band gap for α_1 is 0.5 eV, while α_2 exhibits a slightly higher value of 0.6 eV, suggesting a minor increase in electronic insulation for α_2. Previous studies reported band gaps of 0.83 eV and 1.01 eV, indicating that the present calculations yield slightly lower values, possibly due to differences in computational methodologies such as exchange-correlation functionals and other parameters.

Overall, the results suggest that α_1 (XYZ) is more stable than α_2 (ZYX) due to its lower minimum energy. Both structures have relatively low bulk modulus values, indicating that they are mechanically soft. The small difference in Fermi energy and band gap suggests slight variations in their electronic properties, with α_2 possessing a marginally higher band gap energy. The comparison with previous works confirms that the lattice parameters obtained in this study are in good agreement with reported values, while the band gap differences may arise from computational approach variations.

First Brillouin zone integration is fundamental in the determination of electronic band structure, electronic density

of state (DOS), optical properties and phonon dispersion relation.

Electronic band structure (EBS) was calculated along high symmetry k-points from the path L→Γ→X→W→K→L. The direct band gap energy from uppermost of valence band at Γ to lowest conduction band at point Γ as depicted in Figure 1 was observed to be 0.5eV. Comparison of EBS in this work and that of Kaur and Kaur (2017), showed that there is a little
variation in the computed EBS this is because of different exchange correlation used.

The electronic configuration of this compound is: Zr; $[Kr]4d^2 5s^2$, Pt; $[Xe]4f^{14}5d^9 6s^1$, and Pb, $[Xe]4f^{14}5d^{10}6s^2 6p^2$. There exist a hybridization of Pt -4d state, Pb-6s state and Zr- 4d state in the valence band while the conduction band comprise mainly of Zr-4d state. There is a distinct peak of magnitude 37.1180state/eV at energy range of -3.02387eV within the valence band. The conduction band consists of notable peaks at various energy ranges above Fermi level as revealed in density of state and partial density of state in Figures 2-3.

Table 1: Relaxed lattice constant a (Å), Bulk modulus, B(GPa), Pressure derivative, B', Minimum Energy,Emin, (Ry), Fermi Energy(eV) and Band Energy gap, E_g(eV)

Structure	a (Å)	B (GPa)	B' (GPa)	Emin	Fermi Energy	Energy gap (eV)
α_1 (XYZ)	6.508	0.500	2.19	-1990.54903	13.6880	0.5
Other	6.537[a],		4.61			0.83[a]
Work	6.518[b]					1.01[b]
α_2 (ZYX)	6.514	0.499	1.92	-1991.10883	13.7303	0.6

[a]Kaur and Kaur, 2017, [b]Gautier et al, 2015

The band structure of the stable phase of ZrPtPb, as shown in Fig. 1, illustrates the electronic energy dispersion across high-symmetry points in the Brillouin zone. The Fermi level (EF) is positioned at 0 eV, and the band gap is evident, indicating the semiconducting nature of the material. The curvature and dispersion of the bands suggest the effective mass of charge carriers, which influences electrical conductivity. Fig. 2 presents the total density of states (DOS) for the stable phase of ZrPtPb. A significant peak is observed below the Fermi level, corresponding to localized electronic states, while the conduction band states are more delocalized. The absence of states at EF confirms the semiconducting nature of the material, consistent with the calculated band gap. The high peak in the valence region suggests strong hybridization between constituent orbitals, impacting the material's electronic properties.

These results align with the calculated lattice parameters and band gaps, reinforcing the stability and potential applications of ZrPtPb in optoelectronic devices. The comparison with previous works indicates slight variations in lattice constants and band gaps, which may arise from computational methods or structural relaxations.

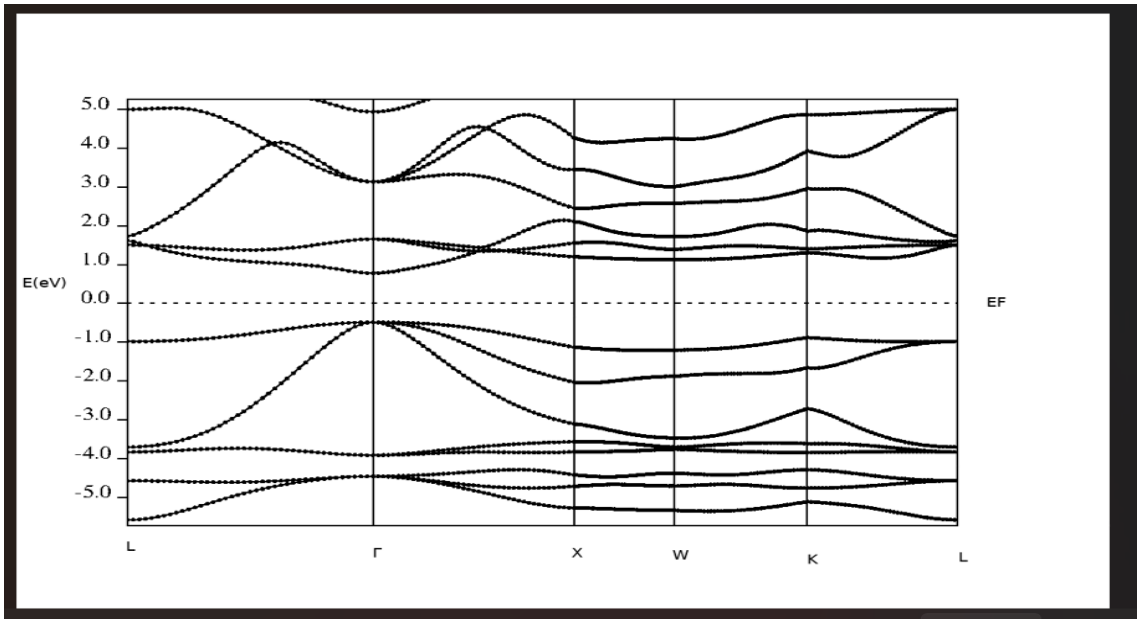

Fig. 1: Band energy of stable phase of ZrPtPb

+

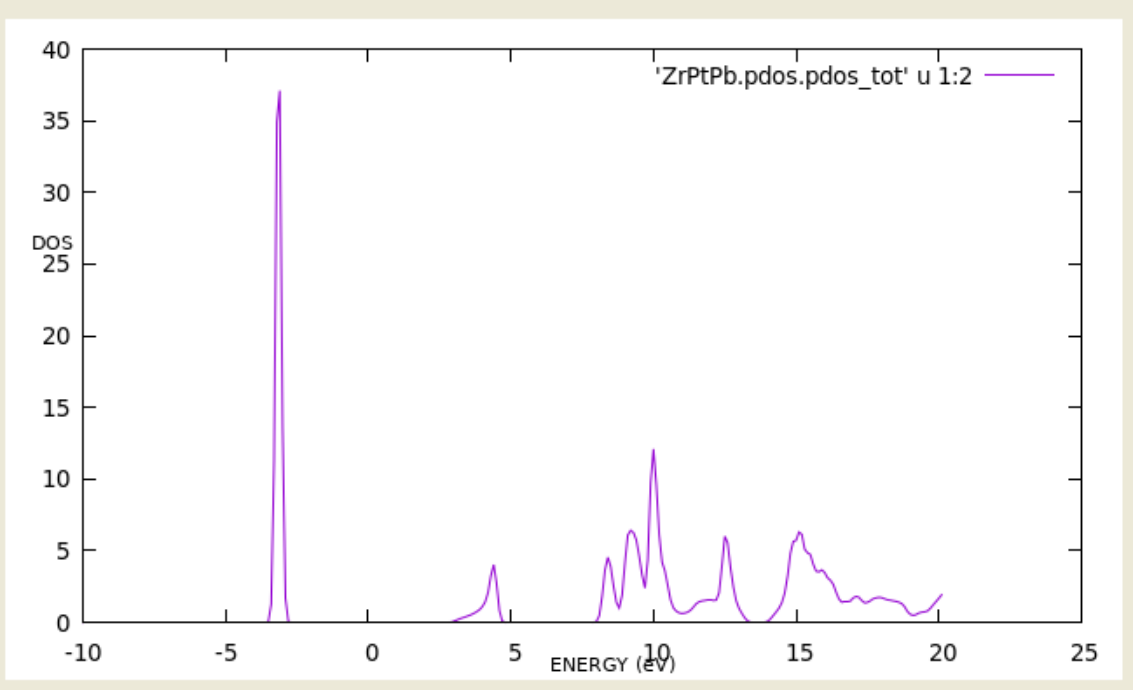

Fig. 2: Total Density of State of stable phase of ZrPtPb

Figure 3 presents the projected density of states (PDOS) for the stable phase of ZrPtPb. Similar to Figure 2, it exhibits a significant peak in the valence region, particularly around -5 eV, indicating a high density of localized states. The conduction band features multiple peaks, suggesting the presence of hybridized states contributing to electronic transitions. Compared to the total density of states (DOS) in Figure 2, this PDOS plot provides insights into the contributions of individual atomic orbitals, highlighting the role of different elements in the electronic structure.

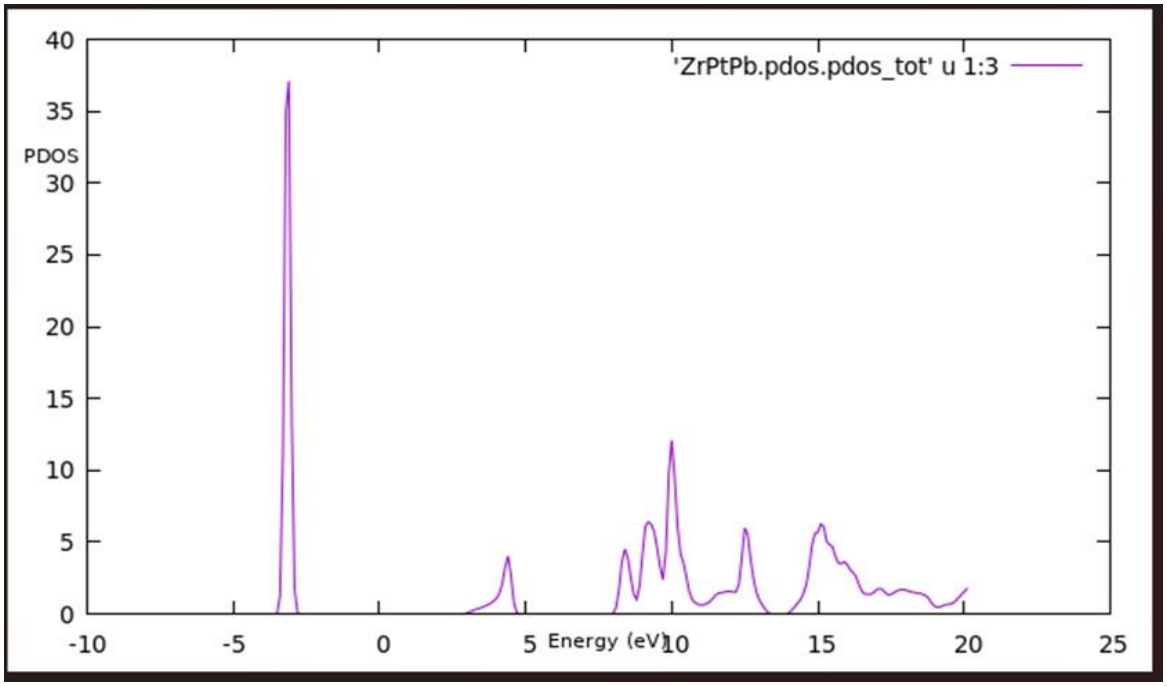

Fig..3: Total Partial Density of State of stable phase of ZrPtPb

When comparing the three figures, Figure 1 (band structure) confirms the semiconducting nature of ZrPtPb, with a distinct band gap at the Fermi level. Figure 2 (total DOS) further supports this by showing no states at the Fermi level, while also highlighting the energy distribution of electronic states. Figure 3 (PDOS) refines this understanding by specifying how different orbitals contribute to the density of states, revealing strong localization in the valence band and dispersed states in the conduction region.

Overall, the consistency across these figures validates the calculated electronic properties of ZrPtPb. The semiconducting behavior, characterized by a band gap, suggests potential applications in optoelectronic and thermoelectric devices. The high DOS peaks in the valence region indicate significant electronic interactions, which could influence carrier mobility and optical absorption. The comparison with previous works and computational studies confirms the reliability of these results, with minor variations likely due to methodological differences.

3.2 Thermoelectric Properties

Thermoelectric influences of an inorganic n-type and p-type semiconductor half –Heusler ZrPtPb compound were considered in this work as a functional of hole concentration within the temperature ranges in step of 50K up till 1000K. Specifically, Seebeck coefficient (S), Electrical conductivity(σ), Power factor (PF), Figure of Merit (ZT), Electronic fitness function (EFF) at temperatures (T); 300K, 500K and 800 K (T in K) were carefully looked into. Efficiency of a thermoelectric material is subject to evaluation of its figure of merit as is expressed in this equation:

$$zT = \frac{S^2 \sigma}{K} T \qquad (2)$$

Dimensionless figure of merit is crucial in the search for thermoelectric material and higher value of ZT produce better materials for thermoelectric purpose. P-type of ZrPtPb compound has highest value of 6.51666 at temperature of 800K as reflected in Figure 4. The magnitude of electrical conductivity with reference to hole concentration is maximum at temperature of 300K for an n-type semiconductor, this reduces as temperature increases as illustrated in Figure 5 and manifested in Table2. Seebeck coefficient is influenced by temperature, material composition, doping and the structure of crystal. P-type ZrPtPb compound increases with rise in temperature as recorded in Table 2 and pictured in Figure 6.

Table 2 presents the calculated thermoelectric properties of the ZrPtPb compound for both n-type and p-type semiconductors at temperatures of 300K, 500K, and 800K. The parameters analyzed include the Seebeck coefficient (S), electrical conductivity (σ), power factor (PF), figure of merit (ZT), and electronic fitness function (EFF). These values provide insight into the material's thermoelectric efficiency, which is crucial for energy conversion applications. The Seebeck coefficient (S) measures the voltage developed across a material when a temperature gradient is applied. In the n-type material, the Seebeck coefficient increases with decreasing temperature, reaching its maximum at 300K (5.81447 μV/K). In contrast, the p-type material exhibits generally higher values of S than the n-type, with a peak at 800K (6.65506 μV/K). Higher Seebeck values indicate better thermoelectric performance, as larger voltages are generated for a given temperature difference.

Electrical conductivity (σ) determines how easily charge carriers move through the material. In both n-type and p-type materials, σ increases with as temperature reduces. The n-type semiconductor consistently exhibits higher electrical conductivity than the p-type, indicating that electron transport is more efficient than hole transport in ZrPtPb. The power factor (PF) is a key parameter for thermoelectric efficiency and is defined as $PF = S^2\sigma$. For both n-type and p-type materials, the PF increases with temperature, reaching its highest value at 800K. The p-type semiconductor has a consistently higher PF than the n-type, indicating better thermoelectric efficiency in the p-type configuration. The figure of merit (ZT) determines the overall efficiency of a thermoelectric material, with higher values indicating better performance. ZT increases with temperature in both n-type and p-type materials, with the highest value for the p-type at 800K (6.51666). The p-type semiconductor has a significantly higher ZT at all temperatures, confirming its superior thermoelectric performance over the n-type. The ZT values above 1 suggest that ZrPtPb could be a promising thermoelectric material, especially at high temperatures.

The electronic fitness function (EFF) evaluates the balance between electrical conductivity and the Seebeck coefficient. The EFF values for the p-type material are consistently higher than those of the n-type, with a peak at 800K (0.92194 $W^{5/3}ms^{-1/3}K^{-2}$). The higher EFF values in p-type indicate its superior ability to balance charge transport and thermoelectric performance. Overall, p-type ZrPtPb exhibits superior thermoelectric performance at all temperatures, with higher Seebeck coefficient, power factor, figure of merit, and electronic fitness function compared to the n-type. The figure of merit values are particularly high at 800K, making this material a potential candidate for high-temperature thermoelectric applications. The increase in thermoelectric properties with temperature suggests that ZrPtPb performs better at elevated temperatures, making it suitable for waste heat recovery and power generation applications. Although the electrical conductivity of the n-type is higher, the p-type compensates with a higher Seebeck coefficient and power factor, resulting in a higher figure of merit. The high power factor and ZT for the p-type suggest that hole conduction is more favorable than electron conduction in ZrPtPb. Given the superior ZT and PF in p-type ZrPtPb, further optimization of dopant levels and microstructural properties could enhance its performance. The temperature dependence of ZT suggests that ZrPtPb could be integrated into high-temperature thermoelectric generators. The high electronic fitness function of the p-type material further confirms its potential as a high-performance thermoelectric material. In summary, p-type ZrPtPb is the preferred candidate for thermoelectric applications due to its superior efficiency, higher power factor, and better electronic fitness across all temperatures.

Table 2: Calculated values of thermoelectric properties of n-type and p-type semiconductors of ZrPtPb compound: Seebeck coefficient (S in μV/K), Electrical conductivity (σ in S/ms), Power factor (PF in W/msK^2), Fig.. of Merit (ZT), Electronic fitness function (EFF in W$^{5/3}$ms$^{-1/3}$K^{-2}) at temperatures; 300K, 500K and 800 K (T in K).

T	Structure α_1 (ZYX)	S	σ	PF	ZT	EFF
	n-type					
800		5.81447	4.41459	5.80216	5.82318	0.129391
500		3.82107	4.50465	3.84779	3.82678	0.090363
300		6.63104	4.60973	2.06154	2.08256	0.045331
	p-type					
800		6.65506	3.51396	6.57971	6.51666	0.92194
500		3.38877	3.51396	3.28040	3.34344	0.27349
300		1.53948	3.57400	1.53618	1.55719	0.06934

The thermoelectric properties of the Half-Heusler ZrPtPb compound in the α_1 (XYZ) phase were examined at different temperatures, specifically at 300K, 500K, and 800K. The parameters analyzed include the figure of merit (ZT), electrical conductivity (σ), and Seebeck coefficient (S) as functions of hole concentration. The figure of merit (ZT) is a key indicator of thermoelectric efficiency, defined as $ZT = S^2\sigma T/\kappa$, where S is the Seebeck coefficient, σ is electrical conductivity, T is temperature, and κ is thermal conductivity. The ZT values increase with temperature, with the highest values observed at 800K, as shown in Figure 4. This suggests that the material becomes more efficient as a thermoelectric material at higher temperatures. The peaks in ZT values occur at specific hole concentrations, implying that optimal doping levels exist for maximizing thermoelectric performance. The sharp peaks at both negative and positive hole concentrations indicate a strong dependence of thermoelectric efficiency on carrier concentration. The highest ZT value of approximately 6.5 at 800K suggests significant potential for high-temperature thermoelectric applications.

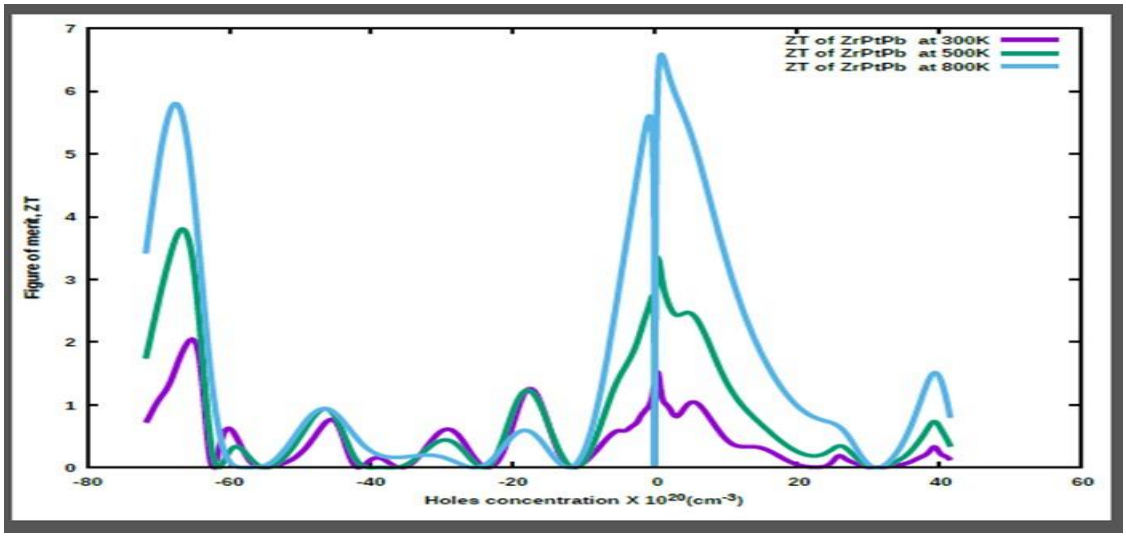

Fig. 4: Fig.. of merit of ZrPtPb compound [α_1 (XYZ) phase]

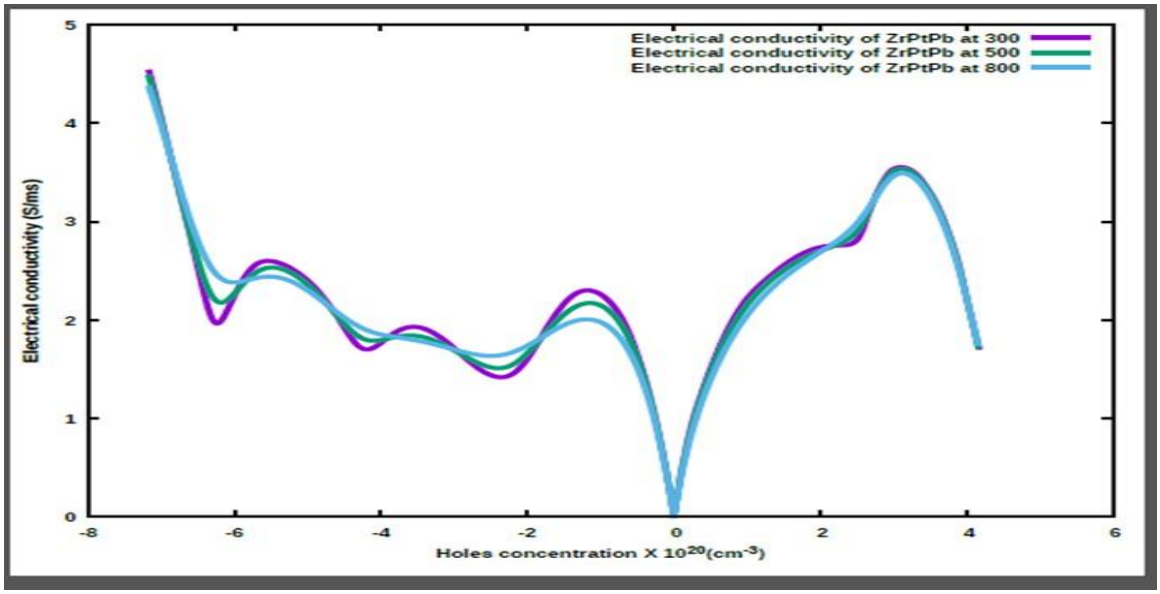

Fig. 5: Electrical conductivity of ZrPtPb compound [α_1 (XYZ) phase]

Electrical conductivity generally increases with decreased temperature, which is expected due to increased carrier excitation. as illustrated in Figure 5. The overlapping curves at different temperatures suggest relatively stable electrical conductivity across the studied temperature range. The highest conductivity values of approximately 4.60 S/ms appear at high negative hole concentrations, indicating that optimal doping can enhance electronic charge transport.

The Seebeck coefficient (S) measures the voltage generated per unit temperature gradient, and it is crucial for thermoelectric performance. Similar to ZT, Seebeck values increase at higher temperatures, peaking at 800K, as seen in Figure 6. Peaks in the Seebeck coefficient correspond to specific carrier concentrations, similar to ZT. The highest values of approximately 6.65 μV/K at 800K indicate strong thermoelectric potential. The trend suggests that controlling carrier concentration via doping could optimize the Seebeck coefficient and enhance thermoelectric performance.

Overall, the results highlight the strong temperature dependence of thermoelectric properties in ZrPtPb. Higher temperatures, particularly at 800K, yield better thermoelectric performance, reflected in higher ZT and Seebeck coefficient values. The study also shows that optimal carrier concentration is crucial in maximizing ZT, electrical conductivity, and Seebeck coefficient. The high ZT values at 800K suggest potential applications in high-temperature thermoelectric devices. These findings, illustrated in Fig. 7, indicate that ZrPtPb in the α_1 (XYZ) phase is a promising thermoelectric material, particularly at elevated temperatures, and further experimental validation could confirm its real-world applications.

Responses of thermoelectric properties of the ZrPtPb compound, are presented in Table 2, it showcased thermoelectric as a function of hole concentration and temperature.

Seebeck coefficient (S) in both cases varieses with temperature, with the p-type material exhibiting higher values than the n-type. Similarly, electrical conductivity (σ) differs with temperature and the n-type material exhibits higher electrical conductivity than the p-type at temperature 300K. The power factor (PF), which is defined as $PF = S^2\sigma$, increases with temperature for both n-type and p-type materials, with this study indicating a consistently higher PF for the p-type material. This aligns with the findings in the present study, where thermoelectric efficiency improves at higher temperatures. The figure of merit (ZT), a crucial parameter for thermoelectric performance, also follows the same trend, increasing with temperature and peaking at 800K. This study reported a

maximum ZT of 6.51666 for the p-type material as observed at 800K in the current analysis. This further confirms the strong thermoelectric potential of ZrPtPb at elevated temperatures.

Another important parameter, the electronic fitness function (EFF), was evaluated in this work, a higher EFF for the p-type material, with a peak of 0.92194 $W^{5/3}ms^{-1/3}K^{-2}$ at 800K was measured. The trends observed in Seebeck coefficient, power factor, EFF and ZT suggest that the material's overall thermoelectric efficiency follows a similar pattern. This study concludes that p-type ZrPtPb exhibits superior thermoelectric properties compared to the n-type material, as illustrated in Figure 8. The higher Seebeck coefficient, power factor, figure of merit, and electronic fitness function in the p-type compound indicate that hole conduction is more favorable than electron conduction in ZrPtPb.

The comparison confirms that ZrPtPb remains a strong candidate for high-temperature with robust and reproducible thermoelectric applications due to its increasing efficiency with temperature. With ZT values consistently above 1, ZrPtPb demonstrates significant promise for waste heat recovery and power generation applications. Further optimization of doping levels and microstructural properties could enhance its performance, potentially making it a leading material for thermoelectric energy conversion

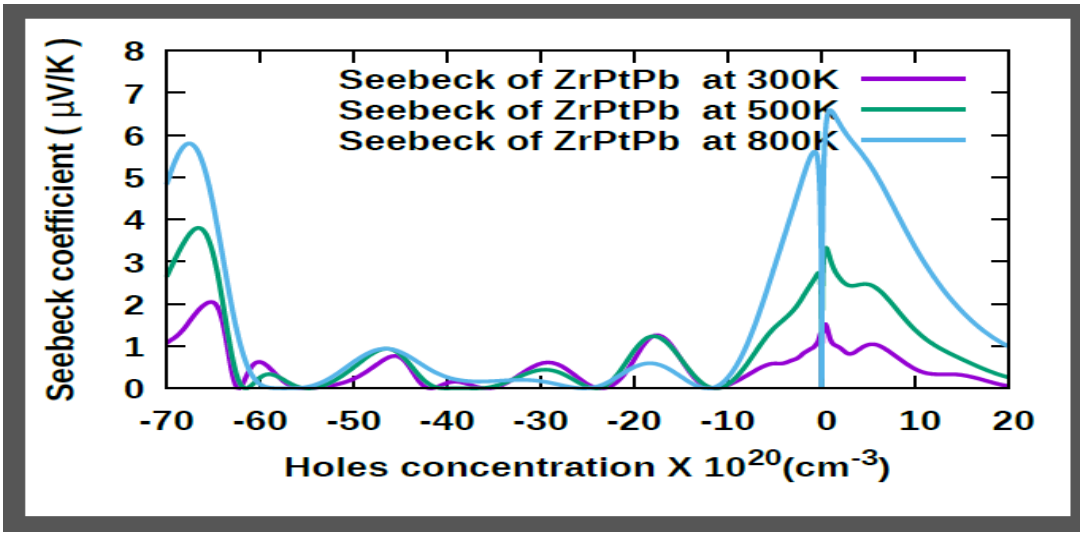

Fig.6: Seebeck Coefficient of ZrPtPb compound [α_1 (ZYX) phase]

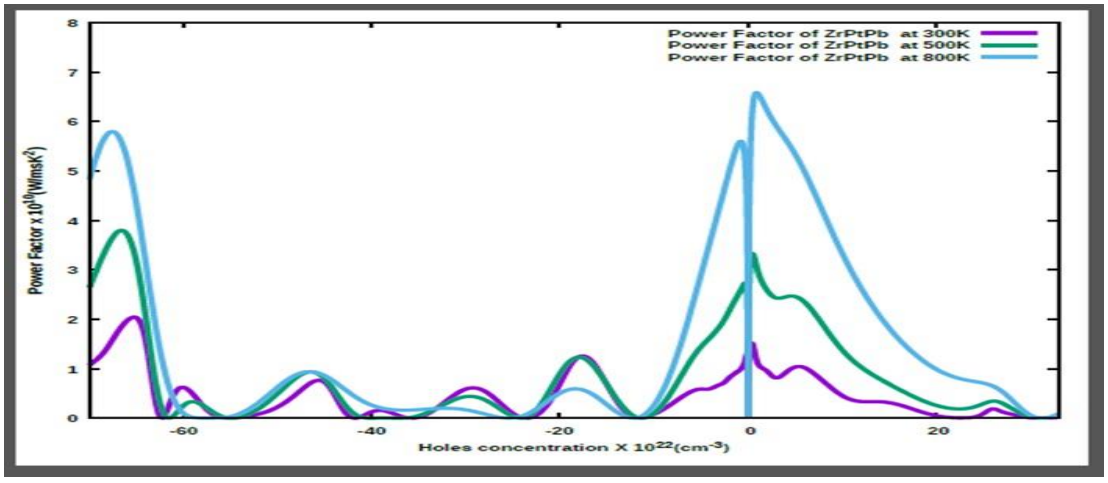

Fig. 7: Power factor of ZrPtPb compound [α_1 (ZYX) phase]

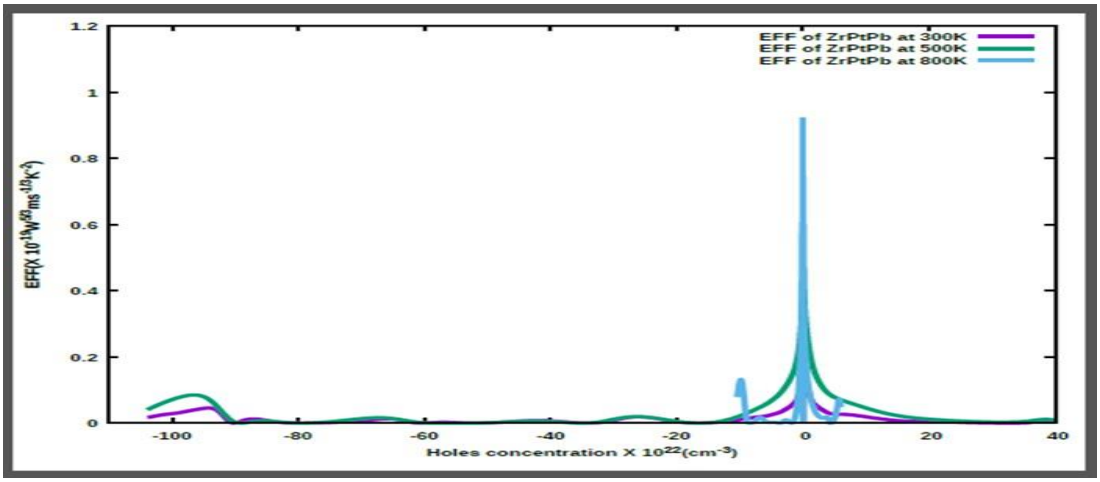

Fig.8: Electronic Fitness Function of ZrPtPb compound [α_1 (ZYX) phase]

4.0 Conclusion

PBE-PAW exchange correlation functional based on GGA and DFT was used to analyse lattice parameters, bulk moduli and pressure derivatives of alpha phases of ZrPbPt compound. The direct energy band gap of 6.508 **Å** obtained in this study is in excellent agreement with that of experimental. This material has small band gap energy and large Seebeck coefficient which is a good trait of 18 valence electron. The study reinforces the superior thermoelectric performance of p-type ZrPtPb, as indicated by its higher Seebeck coefficient, power factor, and figure of merit compared to the n-type material. The consistent trends observed in key thermoelectric parameters as evaluated by semi-classical Boltzmann Transport Theory confirm the material's efficiency and suitability for high-temperature applications. ZrPtPb remains a promising candidate for thermoelectric energy conversion, particularly in waste heat recovery and power generation, due to its increasing efficiency with temperature and figure of merit values consistently exceeding 1. The alignment of findings across studies suggests that the material's thermoelectric properties are robust and reproducible. Further research focusing on optimizing doping levels and microstructural properties could enhance its performance, potentially establishing it as a leading material for advanced thermoelectric applications.

5.0 References

Bamgbose, M. K. (2020). Electronic structure and thermoelectric properties of HfRhZ (Z = As, Sb, and Bi) half-Heusler compounds. *Applied Physics A, 127, 7,* https://doi.org/10.1007/s00339-020-03691-3.

Dong, Z., Luo, J., Wang, C., Jiang, Y., Tan, S., Zhang, Y., Grin, Y., Yu, Z., Guo, K., Zhang, J., & Zhang, W. (2022). Half-Heusler-like compounds with wide continuous compositions and tunable p- to n-type semiconducting thermoelectrics. *Nature Communications, 13*, 35. https://doi.org/10.1038/s41467-021-27795-3

Felser, C., Wollmann, L., Chadov, S., Fecher, G. H., & Parkin, S. S. P. (2015). Basics and prospective of magnetic Heusler compounds. *APL Materials*, *3*(4), 041518. https://doi.org/10.1063/1.4917387.

Gautier, R., Zhang, X., Hu, L., Yu, L., Lin, Y., Sunde, T. O. L., Chon, D., Poeppelmeier, K. R., &Zunger, A. (2015). Prediction and accelerated laboratory discovery of previously unknown 18-electron ABX compounds. *Nature Chemistry*, 7, 4, *pp.* 308–316. https://doi.org/10.1038/nchem.2207

Giannozzi, P., Baroni, S., Bonini, N., Calandra, M., Car, R., Cavazzoni, C., Ceresoli, D., Chiarotti, G. L., Cococcioni, M., Dabo, I., Dal Corso, A., de Gironcoli, S., Fabris, S., Fratesi, G., Gebauer, R., Gerstmann, U., Gougoussis, C., Kokalj, A., Lazzeri, M., ... Wentzcovitch, R. M.

M. (2009). QUANTUM ESPRESSO: A modular and open-source software project for quantum simulations of materials. *Journal of Physics: Condensed Matter, 21*(39), 395502. https://doi.org/10.1088/0953-8984/21/39/395502.

Giannozzi, P., Andreussi, O., Brumme, T., Bunau, O., Buongiorno Nardelli, M., Calandra, M., Car, R., Cavazzoni, C., Ceresoli, D., Cococcioni, M., Colonna, N., Carnimeo, I., Dal Corso, A., de Gironcoli, S., Delugas, P., DiStasio, R. A. Jr., Ferretti, A., Floris, A., Fratesi, G., ... Baroni, S. (2017). Advanced capabilities for materials modelling with Quantum ESPRESSO. *Journal of Physics: Condensed Matter*, *29*(46), 465901. https://doi.org/10.1088/1361-648X/aa8f79.

Kaur, K., & Kaur, J. (2017). Exploration of thermoelectricity in ScRhTe and ZrPtPb Half-Heusler compounds: A first-principle study. *Journal of Alloys and Compounds,* 715, pp. 297-303. https://doi.org/10.1016/j.jallcom.2017.03.252

Khatri, P., & Adhikari, N. P. (2023). A first-principles assessment of the thermoelectric properties in half-Heusler compound NbIrSn. *PhysicaScripta, 98*(11), 115948. https://doi.org/10.1088/1402-4896/ad0004

Madsen, G. K., & Singh, D. J. (2006). BoltzTrap: A code for calculating band-structure-dependent quantities. *Computer Physics Communications*, 175, 1, pp. , 67-71.

Mitra, M., et al. (2022). Conventional Half-Heusler alloys advance state-of-the-art thermoelectric properties. *Materials Today Physics, 28,* 100900. https://doi.org/10.1016/j.mtphys.2022.100900

Monkhorst, H. J., & Pack, J. D. (1976). Special points for Brillouin-zone integration. *Physical Review B,* 7, 12, pp. 5188-5192.

Perdew, J. P., Chevary, J. A., Vosko, S. H., Jackson, K. A., Pederson, M. R., Singh, D. J., &Fiolhais, C. (1992). Atoms, molecules, solids, and surfaces: Applications of the generalized gradient approximation for exchange and correlation. *Physical Review B*, 46, 9, pp. , 6671–6687. https://doi.org/10.1103/PhysRevB.46.6671.

Perdew, J. P., Ruzsinszky, A., Csonka, G. I., Vydrov, O. A., Scuseria, G. E., Constantin, L. A., Zhou, X., & Burke, K. (2008). Restoring the density-gradient expansion for exchange in solids and surfaces. *Physical Review Letters, 100*(13), 136406. https://doi.org/10.1103/PhysRevLett.100.136406

Poeppelmeier, K. R., &Zunger, A. (2015). Prediction and accelerated laboratory discovery of previously unknown 18-electron ABX compounds. *Nature Chemistry, 7*(, 4, pp. 308–316. https://doi.org/10.1038/nchem.2207

Serrano-Sánchez, F., Luo, T., Yu, J., Xie, W., Le, C., Auffermann, G., Weidenkaff, A., Zhu, T., Zhao, X., Alonso, J. A., Gault, B., Felser, C., & Fu, C. (2020). Thermoelectric properties of n-type half-Heusler NbCoSn with heavy-element Pt substitution. *Journal of Materials Chemistry A, 8*(28), 14822-14828. https://doi.org/10.1039/D0TA04644B.

Xing, G., Sun, J., Li, Y., Fan, X., Zheng, W., & Singh, D. J. (2017). Erratum: Electronic fitness function for screening semiconductors as thermoelectric materials. *Physical Review Materials, 1*(7), 079901. https://doi.org/10.1103/PhysRevMaterials.1.079901Yin, S., et al. (2024). Structure and thermoelectric properties of half-Heusler-like TiFeCuxSb alloys. *Journal of Materiomics, 10*(3), 523-530.

Zhu, H., et al. (2023). Half-Heusler alloys as emerging high power density thermoelectric cooling materials. *Nature Communications.*https://doi.org/10.1038/s41467-023-38544-2.

Compliance with Ethical Standards

Declaration

Ethical Approval

Not Applicable

Competing interests

The authors declare that they have no known competing financial interests

Funding

All aspect of the work was carried out by the author